Atmospheric Environment Vol. 24A, No. 11, pp. 2835–2838, 1990
Printed in Great Britain.

0004-6981/90 $3.00 + 0.00
Pergamon Press plc

AN INFRARED METHOD FOR PLUME RISE VISUALIZATION AND MEASUREMENT

CINDY RICKEL, BRIAN LAMB,* ALEX GUENTHER and EUGENE ALLWINE
Laboratory for Atmospheric Research, Department of Civil and Environmental Engineering, Washington State University, Pullman, WA 99164-2910, U.S.A.

(*First received* 10 *February* 1989 *and in final form* 11 *May* 1990)

Abstract—An infrared video camera and recording system were used to record near source plume rise from a low turbine stack at an oil gathering center at Prudhoe Bay, AK. The system provided real-time, continuous visualization of the plume using a color monitor while the images were recorded with a standard video tape recorder. Following the field study, single frame images were digitized using a micro-computer video system. As part of the digitization, the plume centerline was determined as well as an isotherm of the plume outline. In this application, one frame from each 2-min period in the record was digitized. The results were used to calculate the variability in plume centerline during each hour. During strong winds with blowing snow, the mean plume rise for the hour at 15 m downwind was 6 ± 2 m. The observed plume rise from the turbine stack was greater than that calculated using momentum-only or buoyancy-only plume rise models and only slightly larger than that estimated from combined momentum–buoyancy plume rise models.

Key word index: Plume rise, infrared, video, image analysis, Arctic, building dispersion.

1. INTRODUCTION

Maximum pollutant concentrations downwind of industrial complexes are very sensitive to the combined effects of plume rise, plume downwash due to building effects, and building enhanced vertical dispersion. In current air quality models, such as the Industrial Source Complex model, plume rise is calculated using a combined momentum and buoyancy plume rise algorithm, while building effects are parameterized in the treatment of vertical dispersion (see Guenther *et al.*, 1990). Since this parameterization is a function of plume height relative to building height, accurate calculation of plume rise is doubly important for low industrial stacks.

As part of an extensive evaluation of industrial complex modeling methods applied to Arctic oil production facilities, we have conducted a field study of plume downwash and dispersion at an oil gathering center in Prudhoe Bay, AK, during October–November 1987 (Guenther *et al.*, 1990), and we have completed an analysis of wind tunnel tests of the same facility (Guenther *et al.*, 1989). To obtain a direct measure of plume rise during the field study, we employed an infrared video camera and recorder. Huber (1988) has reported on the use of a video system for recording smoke plumes in a wind tunnel, but it appears that this is a novel application of the commercial infrared camera. In this paper, we describe the video system, field measurements, and image analysis methods. The results are used for comparison to current plume rise models as part of our analysis of plume behavior under Arctic conditions.

2. EXPERIMENTAL PROCEDURES

The field study was conducted at an oil gathering center (GC2) shown in Fig. 1 located in the Prudhoe Bay oil field approximately 10 km from the coast of the Arctic Ocean. The test site and meteorological conditions observed during the study have been described by Guenther and Lamb (1989). The area is extremely flat and during the study the tundra was snow covered. Strong winds between 6 and 17 m s^{-1} were fairly common during the study. Thermal stratification was slightly stable (1°C/100 m) from the surface to 10 m. In addition to an open area, multi-level meteorological tower, wind speed and direction were measured from a 33 m tower located on the north side of the complex. SF_6 tracer gas was released from one of the two turbine stacks located on the west side of the complex. Each stack is attached to the

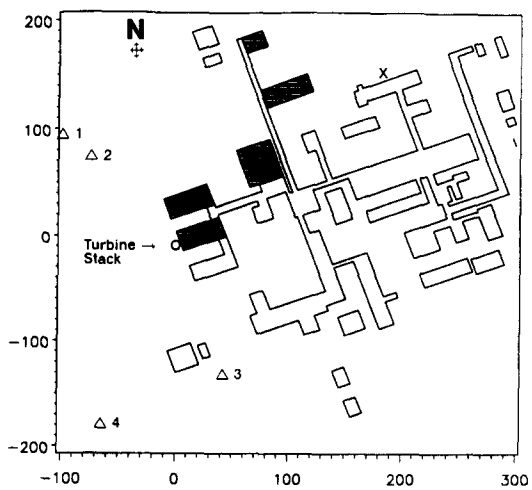

Fig. 1. Map of oil gathering center showing turbine stack (0), meteorological tower (x) and typical camera locations (triangles).

* To whom correspondence should be addressed.

Table 1. System specifications for the PROBEYE 4300 IR video system

Sensitivity	0.1°C
Temperature range	−20 to 280°C
Spectral range	2.0–5.6 μm
Scan rate	16 Hz
Scan lines	60 lines/frame
Field of view	15 horizontal, 7.5 vertical
Focus range	0.2 m to infinity
Spatial resolution	0.126° horizontal and vertical
Scan resolution	256 × 300 pixels

exterior of a large turbine building. The building height was 35 m, stack height was 39 m, and stack diameter was 3.7 m. Winds were from the east during all tests, so that the stacks were located on the downwind side of the oil gathering center. Hourly averaged stack temperature and velocity were measured continuously during the study. Over the 3 week period, stack temperature ranged from 270 to 331°C, and stack gas velocity was in the range 15.6–21.2 m s^{-1}.

The video system was a Hughes model 4300 infrared video camera with a color monitor. Images were recorded continuously using a standard portable video recorder (1/2″ tape). Camera specifications are listed in Table 1. The camera system uses a 16 color scale to depict 16 temperature ranges. The minimum temperature resolution is 0.1°C. The absolute accuracy of the temperature output depends upon using a calibrated emissivity. For our purpose, we assumed an emissivity equal to 1. The extent of the temperature coverage is selected by specifying the temperature of the lowest range. In our application, we optimized the plume image by selecting a minimum temperature slightly less than ambient (typically −20°C) and setting the range width to 1.5°C. With these settings, the edges of the plume were quite distinct, while the central volume of the hot plume appeared as a single color (i.e. the color of the top range).

During each test, the camera was positioned on a tripod outside a van and the monitor and recorder were operated from inside the van. Power was supplied from a 500 w DC/AC inverter from the truck battery. With easterly flow, it was relatively easy to locate the mobile system at a point crosswind to the plume trajectory. Typical camera locations used during these tests are shown in Fig. 1. Time and location were recorded along with camera range settings and the plume image on video tape.

3. DATA REDUCTION AND ANALYSIS

Single frames from each video record were digitized by playing the video tape through a micro-computer video image analysis system (Imaging Technologies, Series 150). One frame was stored from every 2 min of the video record. This provided a reasonable number of images per hour, while keeping the data storage and analysis time within reasonable limits.

For each frame, the operator manipulated the computer screen cursor to draw the stack and the plume centerline on the monitor. Although this is a subjective method for determining the centerline, the plume outlines were quite clear and it was straightforward to draw a line through the approximate center of the plume image. The method was very fast and avoided the need to do any elaborate calculations to find the center of the plume. After the plume centerline was obtained, the operator selected an isotherm value representing the edge of the plume and used the software to display only the plume outline. Both the plume centerline and plume outline were stored for each frame. The results for a typical frame are shown in Fig. 2. In the analysis that follows only the plume centerline data are used. However, it appears that the plume volume data could be used to estimate entrainment and plume growth rates for short distances downwind.

The plume centerline coordinates obtained from the video analysis represent an apparent trajectory which must be corrected for the camera position and the actual direction of the plume travel. The trajectory was converted to real distance units by using the known stack diameter as a distance scale.

Estimates of true plume height were determined using methods outlined by Halitisky (1961) and Fanaki and Lesins (1975). In this approach, the actual plume height and distance along the plume trajectory are calculated using the horizontal distance from the camera to the stack base, measured from a detailed map of the site, the known stack height, the appropriate 5-min average wind direction measured immediately upwind of the stack on a 33 m tower, and the horizontal angle between the camera view axis and the mean wind direction. Halitisky (1961) has shown that for cases where the camera view axis is within approximately 20° of perpendicular to the mean wind direction, errors associated with the calculated plume rise are less than approximately 25% even if the correction for wind angle is omitted. During each test, the camera position was chosen so that the view axis was close to perpendicular to the plume transport direction. This was possible because the winds were very steady with hourly values of σ_θ typically less than 8°. Halitsky (1961) also showed that horizontal wind direction fluctuations less than ±20° produced errors in the calculations of less than approximately 10%.

The accuracy of the observed plume trajectory depends upon the accuracy of the camera location relative to the stack, the accuracy of the observed wind direction, and the accuracy of the apparent plume

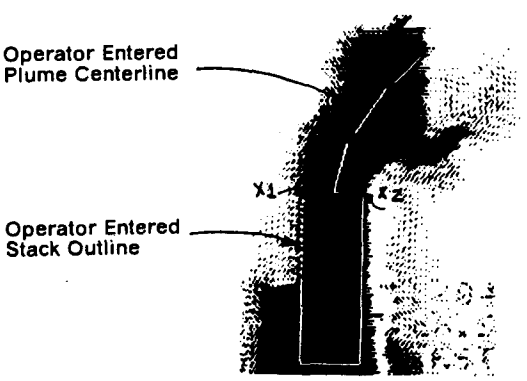

Fig. 2. Typical plume image showing the stack outline, plume boundaries, and plume centerline.

trajectory obtained from the image of the plume. In the first case, camera location was easily obtained to within 5 m from locations recorded on a detailed map. This corresponds to less than 5% of the distance of the camera from the stack. Wind directions appear to be correct to within 2–3° based upon comparison with other measurements and upon the ground-level location of the observed maximum tracer concentration. The vertical range of the plume volume was typically of order 5–10 m so that within this range the plume centerline can be correctly positioned to within approximately 2 m.

Typical results from the plume rise measurements are shown in Fig. 3 for an hour from test 10 of the study. Winds during this period were 14 m s^{-1} from 51° measured at 10 m above the surface. The stack temperature was 295°C and stack gas velocity was 19.4 m s^{-1} for the hour. The data points in Fig. 3 represent plume centerline points at various downwind distances for various instantaneous scans obtained every 2 min during the hour. The scatter of points thus describe the domain of the plume center during the hour. With a mean plume rise of approximately 6 m at 15 m downwind, the plume center varied between approximately 4–8 m above the stack during the hour.

For comparison, Fig. 3 also includes the calculated plume rise based upon momentum-only, buoyancy-only, and combined momentum–buoyancy plume rise models. These are taken from Briggs (1984):

$$h_m = (3F_m X / B_m^2 U^2)^{1/3} \quad (1)$$

$$h_b = 1.6F_b^{1/3} X^{2/3} / U \quad (2)$$

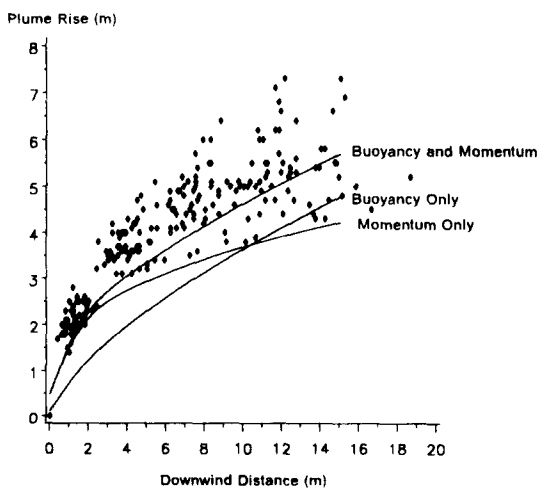

Fig. 3. Observed plume centerline data points (diamonds) from instantaneous scans taken every two minutes during test 10, 1100–1200 AST in comparison to predicted momentum only, buoyancy only, and combined momentum–buoyancy plume rise models.

$$h_{mb} = \left[\frac{3F_m X}{B_m^2 U^2} + \frac{1.6F_b X^2}{B_b^2 U^3} \right]^{1/3} \quad (3)$$

where F_m is the momentum flux, $(=\rho_s(vr)^2/\rho_a)$, B_b is a buoyancy entrainment factor $(=0.6)$, B_m is a momentum entrainment factor $(=0.4+1.2u/v)$, u is the ambient wind speed, v is the stack gas velocity, F_b is the buoyancy flux $=vr^2(T_s-T_a)/T_s$, T_s is the stack temperature, T_a is the ambient temperature, r is the stack radius, ρ_a is ambient air density, ρ_s is stack exhaust density, and x is the downwind distance.

For the hour shown in Fig. 3 and for all other hours with data available, the calculated plume rise based upon momentum only or buoyancy only is less than the lower bound of the observed plume centerlines near the stack. The combined momentum–buoyancy plume rise model slightly underestimates the average observed plume centerline. In other hours, the combined plume rise model underestimated the hourly averaged observed plume rise by 17–38% at short distances from the stack. It is significant that these models underestimate the observed plume rise near the stack even though the models do not account for any plume downwash due to stack or building effects. It is possible that for this near stack domain, the mean streamlines of air passing over the building are still rising and actually carrying the plume upward in this region. It is not possible from the available data to determine the likelihood for this streamline effect. Another possibility to explain the differences between observed and predicted plume rise is that plume rise is enhanced by the close position of two turbine stacks (20 m apart). However, at these small downwind distances, the observed image of the two plumes showed no evidence of the merger needed to produce enhanced plume rise. A third possibility to explain the gap between observed and predicted plume rise is that the large roof-top heat exchangers on the turbine buildings released sufficient volume of warm air to cause enhanced plume rise. Although the warm air from the turbine roof vents was not apparent in the infrared image, it is possible that entrainment of this warm air into the turbine plumes could cause the plumes to rise several meters higher than predicted near the stacks.

4. SUMMARY AND CONCLUSIONS

A unique method for visualizing near stack behavior of plumes has been used to determine plume rise from a turbine stack at an Arctic oil production facility. Because the plume gases are very hot and ambient temperatures are quite cold, the infrared signature of the plume produces a clear image which can be recorded with a commercial infrared video camera. The major limitation of the approach is the relatively short downwind distances over which the plumes can be visualized. However, for the case where plume downwash may be important due to stack or

building effects, the ability to measure initial plume rise is quite useful for interpreting observed tracer gas concentrations downwind of the stack at ground-level. In our application of this visualization system, we observed plume rise during very strong wind conditions which was approximately 1 m higher than predicted from a combined momentum-buoyancy plume rise model at 15 m downwind of the stack.

Acknowledgements—This work was funded by the U.S. Environmental Protection Agency (USEPA) (CR812775-01). The contents of this paper do not necessarily reflect the views and policies of the USEPA, nor does mention of trade names or commercial products constitute endorsement or recommendation for use.

REFERENCES

Briggs G. (1984) Plume rise and buoyancy effects. In *Atmospheric Science and Power Production* (edited by D. Randerson) NTIS DE84005177. Springfield, VA.

Fanaki F. and Lesin G. (1975) Photographic measurement of smoke plume heights from industrial heights. *J. Soc. Motion Picture Television Eng.* **84**, 77–81.

Guenther A. and Lamb B. (1989) Atmospheric dispersion in the Arctic: winter-time boundary-layer measurements, *Boundary-Layer Met.* **49**, 339–366.

Guenther A., Lamb B. and Allwine E. (1990) Building wake dispersion at an Arctic industrial site: field tracer observation and plume model evaluations. *Atmospheric Environment* **24A**, 2329–2347.

Guenther A., Lamb B. and Petersen R. (1989) Plume downwash and enhanced diffusion near buildings: comparison to wind tunnel observations for an arctic industrial site. *J. appl. Met.* **28**, 343–353.

Halitsky J. (1961) Single-camera measurement of smoke plumes. *J. Air Pollut. Control. Ass.* **4**, 185–198.

Huber A. (1988) Video images of smoke dispersion in the near wake of a model building. Part I. Temporal and spatial scales of vortex shedding. *J. Wind Eng. Ind. Aerodyn.* **31**, 189–223.